Solvent-Separated Radical Ion Pairs and Free Ion Yields. 1. Effect of Temperature on Free Ion Formation in Solution

Cheng Zhong, Jinwei Zhou,* and Charles L. Braun*

Department of Chemistry, 6128 Burke Lab, Dartmouth College, Hanover, New Hampshire 03755

Received: February 4, 2004; In Final Form: May 26, 2004

Free ion yields from geminate ion pairs formed after photoinduced electron transfer are measured by the transient photocurrent method in three moderately polar solvents. Photoexcited 9,10-dicyanoanthracene (DCA) is used as the electron acceptor and alkyl-substituted benzenes as donors. It was found that, generally, there is no significant change in free ion yield as the temperature is increased. On the basis of a theoretical model developed under Collins−Kimball boundary conditions, several factors are analyzed, including dielectric constants and viscosities of solvents, initial separation distance distribution of geminate ion pairs, and temperature-induced changes in recombination rates. By comparing escape probabilities of geminate ion pairs calculated at different initial formation and recombination/separation distances with measured free ion yields, we show that free ions are mainly produced from the solvent-separated ion pairs that are initially formed after electron transfer quenching of photoexcited DCA. Calculations also imply that recombination via electron tunneling at separation distances of about 7.5 Å can be considered as the main decay process for solvent-separated ion pairs. There is a direct competition between tunneling recombination and further separation of ion pairs at each distance. Experimental photocurrent rise times indicate that the change in temperature has very limited influence on the recombination rates. On the other hand, an increase in temperature will decrease the viscosities of the solvents and thus increase the mobility of cations and anions significantly, which will, in turn, increase the escape rate and free ion yields. Quantitative analysis indicates that the observed weak dependence of free ion yields on temperature can be attributed to an unfavorable contribution from the decreased dielectric constant at higher temperature.

Introduction

In homogeneous solutions, when the ions are highly charged or very small, or in a weakly polar solvent with a dielectric constant of 20 or less, replacement of solvent molecules or oppositely charged ions that are in contact with the ions concerned could be fairly slow.[1] Winstein et al. demonstrated in their solvolysis study that two kinetically distinguishable ion pairs, intimate (i.e., contact ion pairs) and solvent-separated ion pairs, exist.[2] Bimolecular photoinduced electron-transfer from a donor to an acceptor molecule is an efficient way to produce geminate radical ion pairs or exciplexes. It was found that both emission quantum yields and exciplex lifetime decrease as the solvent polarity increases. However, the polarity-induced decrease of the yields is more significant than the lifetime change. Thus, in the pioneering work of Weller et al., the concepts of contact radical ion pairs (CRIPs) and solvent-separated radical ion pairs (SSRIPs) are introduced.[3]

Intermolecular electron-transfer reactions between donor and acceptor molecules in homogeneous liquid solutions are complicated. The population and the fate of CRIPs and SSRIPs after photoinduced electron-transfer quenching are determined by the properties of the donor and acceptor molecules such as redox potentials and molecular structures, and by the structure and properties of solvents. Our knowledge about the dynamics of CRIPs, SSRIPs, and free radical ion (FRI) formation is limited. Over the past few decades, many studies have been conducted to establish the fundamental mechanism of photoinduced electron transfer in solutions and to test the validity of Marcus theory in these processes.[3,4] Although a general understanding of electron transfer in solution is in hand, many specific problems remain. For example, it is still unclear where (radii) the initial geminate ion pairs are formed after electron transfer quenching of excited electron acceptor (or donor) molecules by electron donors (or acceptors). In other words, we do not know the ratio of CRIPs and SSRIPs when they are initially formed. That, in turn, limits our ability to analyze the mechanism of the decays of both CRIPs and SSRIPs and the formation of free radical ions. It is believed that, in polar solvents such as acetonitrile, SSRIPs are important intermediates with high formation efficiencies after photoinduced electron-transfer quenching.[3,5] In nonpolar solvents such as hexane, CRIPs are the dominant intermediates.[3,6]

Free radical ions are key species for many important processes in solution,[7] liquid crystal[8] and solid.[9] Generally speaking, the free radical ion yields for geminate radical ion pairs formed after electron transfer quenching are determined by recombination rates and escape rates. The escape rate of an ion pair is determined by many factors including separation distance, the diffusion coefficients of both radical cation and anion, dielectric constant of the solvent and the separation distance at which recombination takes place. Unlike the photoexcitation in the charge transfer (CT) band of EDA complexes, which is believed to form only CRIPs,[4,10] photoinduced bimolecular electron-transfer quenching results in the direct formation of both CRIPs and SSRIPs.[3,5] It was found that, for a given donor/acceptor combination, the FRI yield produced by electron transfer

* To whom correspondence should be addressed. E-mail: Charles.L.Braun@Dartmouth.Edu or Jinwei.Zhou@Dartmouth.Edu. Fax: (603)-646-3946.

10.1021/jp049486m CCC: $27.50
Published on Web 07/24/2004

quenching is significantly higher than that by photoexcitation in the CT band.[5a] This implies that no fast equilibrium occurs between CRIPs and SSRIPs before free radical ion formation. In other words, free radical ion formation takes place before CRIPs and SSRIPs formed by forward electron-transfer relax to a common equilibrium state. However, in the recent work of Muller et al.,[11] it was observed that deuterium isotope-induced increases in the fluorescence lifetimes of CRIPs and free ion yields formed after electron-transfer quenching are of the same magnitude. They concluded that free ion formation and charge recombination are in direct competition at contact separation and SSRIPs do not play a significant role in charge separation. This conclusion is in agreement with a model proposed by Mataga et al.[12] that photoinduced electron transfer can happen only at contact separation and forms CRIPs exclusively. It means that free ion formation and decay of the contact CRIPs (or exciplex) can be understood as arising from a single species following two different pathways after photoinduced electron-transfer quenching.

In our previous work, we reported unusual differences in lifetimes of geminate ion pairs as measured by the transient photocurrent technique and single-photon-timing fluorescence after electron-transfer quenching.[13,14] We concluded that there are energy barriers between CRIPs and SSRIPs that appear to be high enough to prevent fast equilibrium between them. We have suggested that the two types of ion pairs have different recombination mechanisms. To acquire further information about the relative energies of CRIPs and SSRIPs and free radical ion formation, transient photocurrent experiments were conducted at different temperatures. In this work, temperature effects on solvent properties and their implications in radical ion pair recombination and free ion formation are analyzed in the framework of model developed by Hong and Noolandi[15] and Sano and Tachiya.[16] This allows determination of the critical recombination/separation distance between donor cations and acceptor anions.

Experiments

All reagents were purchased and used as received except hexaethylbenzene, which was recrystallized in toluene before use. 9,10-Dicyanoanthracene (DCA) from Aldrich was used as the acceptor. Donors used were durene (DUR; Aldrich, 98%), 1,2,4,5-tetraisopropylbenzene (TIPB; Aldrich 96%), hexamethylbenzene (HMB; Aldrich 99%), and hexaethylbenzene (HEB; Aldrich). Solvents used were 1,2-dichloroethane (DCE; Fischer 99%), 3-pentanone (PT; Aldrich; >99%), and 4-methyl-2-pentanone (MPT; Aldrich, >99%).

SCHEME 1: Structures of Donors and the Acceptor Molecule

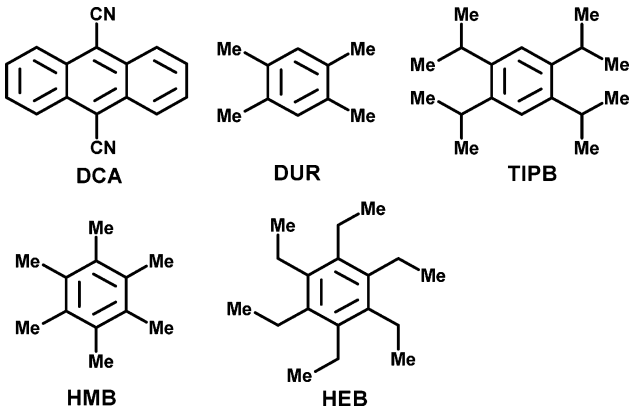

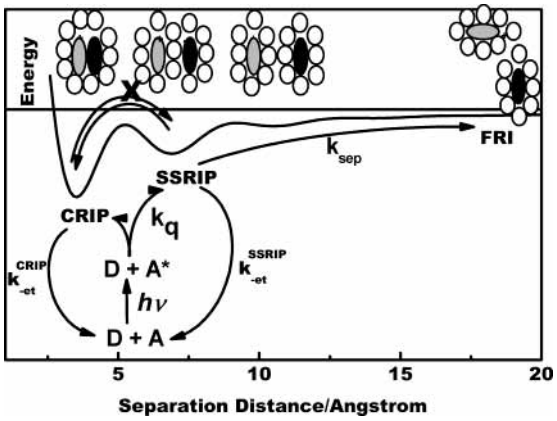

Figure 1. Schematic illustration of ion pair potential energy versus separation.

A detailed description of the method used for transient photoinduced current measurement can be found in our previous work.[17,18] A homemade insulated box was used as a heated enclosure for the photocurrent cell. The temperatures measured were from 293 to 333 K at 10 K intervals with ±1 K uncertainties. Absorbance of the solutions used in the photocurrent experiments was about 0.6 at 355 nm in a 1 cm cell. Concentrations of donors were 0.1 to 0.2 M. The concentration of DCA was 2×10^{-4} to 4×10^{-4} M. A 355 nm pulse from an Orion SB-R laser was used for excitation of the acceptor (DCA) in solution, which was continuously recycled during the measurements. The pulse width was 0.8 ns at a repetition rate of 4 Hz. For the systems measured, a better than 0.5 ns time resolution can be achieved. Pulses had average energies of about 30 μJ. Steady-state fluorescence spectra of DCA in three solvents were measured with a Shimadzu RF-1501 spectrometer before and after the quenching donors were added to normalize the FRI yields to 100% quenching. Single-photon-timing fluorescence experiments were carried out at the same temperatures as photocurrent measurements, which were controlled using a heated cell-holder with a RM6 water-cycling system. A detailed description of the single photon system can be found in our previous work.[14] The pulse width and the effective time resolution of the system are 0.8 and 0.1 ns, respectively. The software used to collect fluorescence decay data was EG&G Maestro32.

Results and Discussion

In our recent work, free ion formation was monitored by a transient photocurrent experiment. Decay of CRIPs was measured by single-photon timing of exciplex emission decay.[14] Generally we found that the two methods gave different lifetimes. Such a difference in lifetimes was also observed by Mataga et al.[19] However, as was discussed above, it could not be understood from their model. We concluded that free radical ions are formed from SSRIPs rather than CRIPs, which give exciplex emission. The rise time of the photocurrent is connected to the decay of SSRIPs, whereas the decay time of fluorescence monitors the decay of CRIPs. The clear difference between the two important time scales shows that there is a local minimum in the potential surface at the position of SSRIPs (Figure 1). A significant barrier exists between CRIPs and SSRIPs that prevents fast equilibrium between them. On the basis of the analysis of the driving force dependence of recombination rate constants of SSRIPs, we suggested[14] that the dominant mechanism for the recombination of SSRIPs involves a direct return electron transfer from SSRIPs by tunneling, thus by-passing the

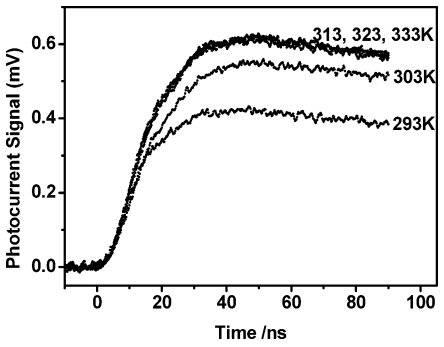

Figure 2. Photocurrent following electron-transfer quenching of excited DCA by TIPB at different temperatures in DCE. The pulse energies that produce geminate ion pairs are normalized to 10 μJ at 355 nm.

CRIPs. We expect that the results from temperature dependence experiments can provide more information on the detailed mechanism of the decay of SSRIPs.

In principle, the decay of SSRIPs can proceed by one of the following three pathways: (a) Direct recombination to ground state with a rate constant k_{-ET}^{SSRIP}, which can be estimated by Marcus theory.[20] Given the fact that the recombination process is in the Marcus inverted region, a stronger donor will have a higher recombination rate. (b) Collapse to CRIPs, followed by decay to the ground state by radiative or nonradiative charge transfer. The collapse is a diffusive process in the Coulomb field of the two ions. The height of the potential barrier between SSRIPs and CRIPs is determined by the desolvation energy. (c) Further separation into free ions via diffusion. Similar to (b), the separation rate constant (k_{sep}) should exhibit very weak dependence on donors in a given solvent if the donors have similar structures and molecular sizes. As will be discussed later, the rate constants of pathways a and b are expected to exhibit different temperature dependences. A careful analysis of the transient photocurrent and exciplex decay results at different temperatures will allow us to evaluate the relative contributions of pathways a and b.

The electron-transfer quenching of the photoexcited acceptor (DCA) by substituted benzene donors was studied in the present work. Free radical ion yields (Y_{FRI}) are measured in three solvents: 3-pentanone (PT), 4-methyl-2-pentanone (MPT), and 1,2-dichloroethane (DCE). The donors used in the experiments were chosen so that, for each of the bulky donors, there is a corresponding less sterically hindered (flat) molecule with nearly identical electron redox potential.[21] The only difference between each pair of the sterically bulky and flat donors is that the flat donors can get closer to the acceptor than can the bulky ones. DCA is a weak electron acceptor ($E°_{Red}$: -0.91 V vs SCE in dichloromethane).[22] For a solution of DCA with the various donors used, excitation at 355 nm results in the almost exclusive formation of excited DCA, which is then quenched by the donor molecule via electron transfer. When bulky donors such as TIPB and HEB are used for the quenching, the radical ion pairs formed do not show any detectable emission. The radical ion pairs thus formed can produce free radical ions effectively. Figure 2 exhibits the photocurrent curves after electron transfer quenching of excited DCA by TIPB at different temperatures in DCE. The rise times were extracted from the apparent exponential increase of the photocurrent signals following excitation. As we have discussed, the rise times can be roughly understood as the lifetimes of SSRIPs.[14] Y_{FRI} can be calculated from the maximum photocurrent signal as it reaches constancy.

When the flat donor DUR, which has similar electronic properties to TIPB, is used, exciplex emission from CRIPs after

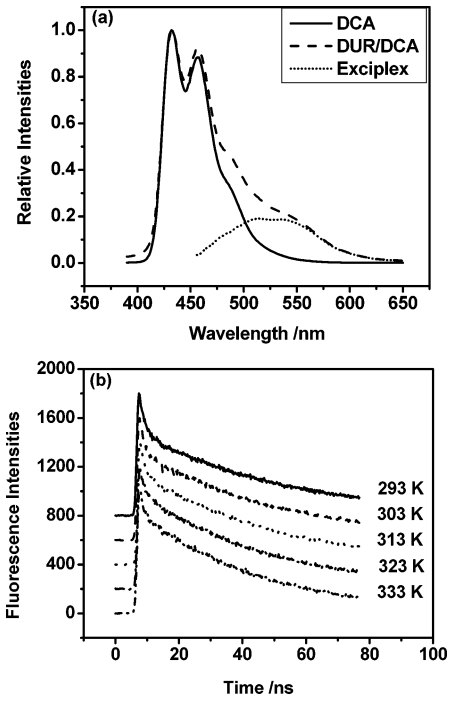

Figure 3. (a) Emission spectra of 2.0×10^{-5} M DCA in the absence and presence of 0.1 M DUR after excitation at 355 nm. The exciplex emission spectrum is obtained by subtracting the DCA emission without DUR from the DUR−DCA emission spectrum. (b) Temperature dependent formation and decays of CRIPs of DUR−DCA in DCE monitored at 580 nm by single-photon counting after excitation at 355 nm.

TABLE 1: Photocurrent Risetimes for TIPB−DCA and DUR−DCA and Fluorescence Decay Times of CRIPs of DUR−DCA in DCE at Different Temperatures

	photocurrent rise time (ns)		exciplex fluorescence
temp, K	TIPB−DCA	DUR−DCA	lifetime (ns) DUR−DCA
293	8.9	24	48
303	10.5	25	46
313	11.1	24	45
323	11.2	23	42
333	10.8	24	40

electron-transfer quenching appears (Figure 3a). The formation and the radiative decay processes of CRIPs can be detected by the single-photon-timing technique (Figure 3b). Similarly, decay of SSRIPs and Y_{FRI} for DUR−DCA can be determined by transient photocurrent experiments at different temperatures. Photocurrent rise times and radiative CRIPs decay times for DCA/DUR are collected in Table 1. For comparison, HMB, a stronger electron donor than DUR, and HEB, a bulky donor with redox potential similar to that of HMB, are used as the DCA quenchers. The free ion yields of DCA with four donors above (DUR, TIPB, HMB, HEB) in DCE at different temperatures are collected together in Table 2a. It should be mentioned that the flat donors, DUR and HMB, are more efficient quenchers than are the corresponding bulky donors, HMB and HEB. At the donor concentration of about 0.1 M used in the photocurrent experiments, about 95% of fluorescence emission from locally excited DCA is quenched by the flat donors, DUR and HMB, whereas only about 80% of the fluorescence emission was quenched by the bulky donors, TIPB and HEB. In Table 2a, all yields shown are normalized to per quenching event rather than per photon. Note that measured Y_{FRI} of all systems show similar very weak temperature dependence as temperature is increased from 293 to 333 K (Figure 4a). Interestingly, the

TABLE 2: Y_{FRI} of Four D/A Systems at Different Temperatures in 1,2-Dichloroethane, 4-Methyl-2-pentanone, and 3-Pentanone

temp, K	DUR	TIPB	HMB	HEB
		a. DCE		
293	0.008	0.088	0.006	0.089
303	0.010	0.098	0.007	0.109
313	0.009	0.093	0.008	0.090
323	0.011	0.090	0.008	0.113
333	0.011	0.086	0.009	0.112
		b. MPT		
293	0.049	0.204	0.017	0.185
303	0.055	0.237	0.021	0.221
313	0.060	0.254	0.024	0.244
323	0.061	0.249	0.025	0.245
333	0.062	0.219	0.025	0.242
		c. 3-PT		
293	0.128	0.226	0.052	0.200
303	0.140	0.204	0.058	0.214
313	0.142	0.230	0.065	0.182
323	0.137	0.225	0.064	0.174
333	0.135	0.196	0.066	0.164

lifetimes of CRIPs between flat donor DUR or HMB and DCA exhibit also only weak temperature dependence. For a temperature increase from 293 to 333 K, the lifetime of CRIPs of DUR−DCA decreases from 48 to 40 ns.

The temperature dependence of Y_{FRI} of all four D/A systems is also studied in solvents such as MPT and 3-PT that are of higher polarity than DCE (Table 2b,c). An important feature of these results is that, as the temperature increases, no significant change in Y_{FRI} can be observed (Figure 4b,c). Another feature of the results is that Y_{FRI} values with bulky donors are much larger than those with flat donors in all systems. More specifically, in a less polar solvent like DCE, the yields using HMB and DUR are about 10 times smaller than those using HEB and TIPB, whereas in relatively more polar solvents such as MPT and 3-PT, the difference is only about 2−4 times.

The primary evidence we presented in our previous work shows that, in moderately polar solvents such as those used in the present work, free radical ions are mainly formed from long distance radical ion pairs that are initially formed by either electron-transfer quenching[13,14] or direct excitation in the CT band of the EDA complexes.[23] We hoped that the temperature dependence experiments would provide further evidence in this regard. The temperature dependence of free ion formation can result from effects on the initial separation distance distribution when RIPs are formed, or from effects on the recombination and separation rates. The recombination rate can be determined experimentally from the rise time of the photocurrent. Thus Y_{FRI} values at different temperatures become direct measures of the temperature dependence of the separation rate (or escape rate). The interaction between cations and anions among RIPs formed is mainly Coulombic in nature.[24] Therefore, the temperature-induced change in dielectric constant has a more significant impact on the escape process of RIPs at short separation distance than at long separation distance. On the basis of this consideration, we expect that Y_{FRI} values and their temperature dependence can be used to probe the initial separation distance of RIPs that contribute to the formation of free radical ions.

To determine the contribution of temperature-induced changes in the physical properties of the solvents, the effects of temperature on viscosities and static dielectric constants of all three solvents are analyzed. The effect of temperature on free ion formation is complicated. Many physical properties of solvents that affect the forward electron transfer, recombination and escape processes are influenced by the temperature of the solution. Viscosity and dielectric constant are two key factors that affect the electron transfer and free ion formation processes. In Table 3 literature values of the viscosities of 1,2-dichloroethane and 3-pentanone over the experimental temperature range are given. In most cases, the dependencies of viscosities on temperature are described as polynomial functions.

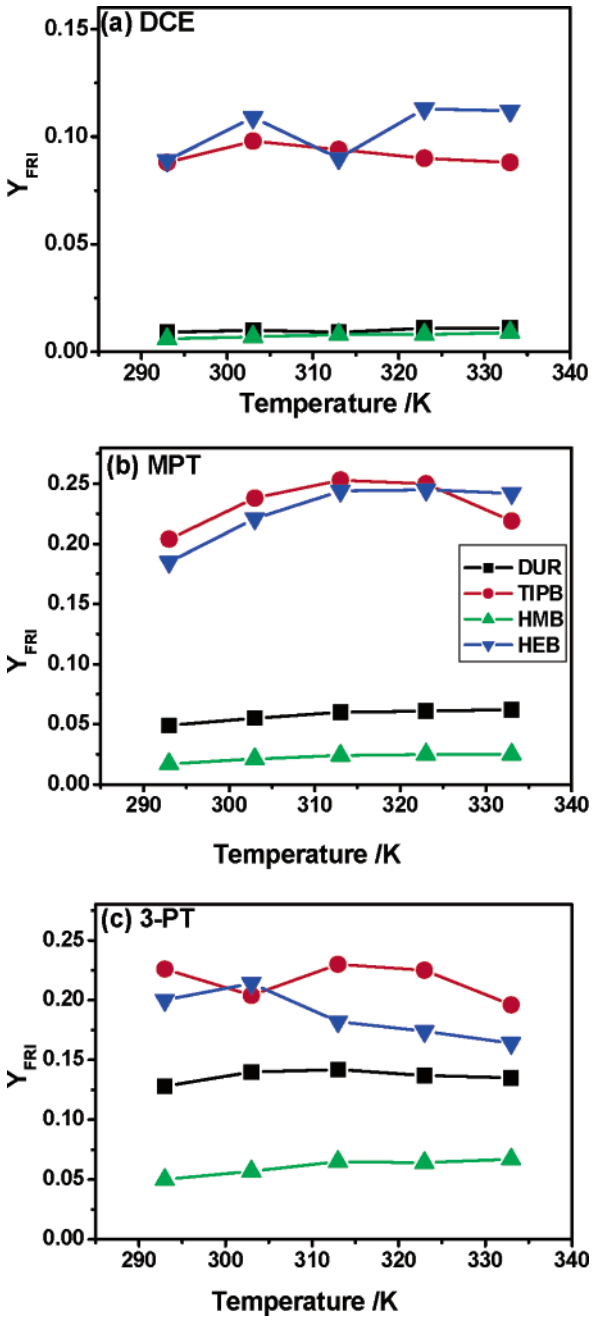

Figure 4. Free radical ion yields (Y_{FRI}) of geminate ion pairs formed by electron-transfer quenching of excited acceptor DCA by four donors at different temperatures in three solvents. The quantum yields are normalized to per quenching event rather than per photon. Key: (●) DUR; (●) TIPB; (●) HMB; (●) HEB.

a. Viscosity. The radical ion pairs separate via diffusion through the solvent molecules while overcoming the Coulomb force between them to form free ions. The diffusion velocity is determined by the solution viscosity, which is required for calculation of ion formation rates and final yields. As we will discuss later, considering the two possible recombination channels, solution viscosity does not affect the through-tunneling recombination process.

TABLE 3: Refractive Indices and Viscosities of the Solvents at Different Temperatures

		293 K	303 K	313 K	323 K	333 K
viscosities,[a] mPa s	PT	0.592	0.444	0.345	0.276	0.221
	DCE	1.125	0.779	0.576	0.447	0.352
static dielectric constants[b]	PT	17.1	16.4	15.7	14.9	14.1
	DCE	10.4	9.9	9.4	8.9	8.5

[a] The viscosity data from *CRC Handbook of Chemistry and Physics*, 83rd ed.; CRC Press: Boca Raton, FL, 2002−2003. [b] The static dielectric constants are calculated from polynomial functions given by the *CRC Handbook of Chemistry and Physics*, 84th ed.; CRC Press: Boca Raton, FL, 2003−2004.

Using a space-filling spherical model, the diffusion constant is calculated by

$$D = \frac{k_B T}{6\pi r_d \eta} \tag{1}$$

where D is the diffusion constant, η is the viscosity of the solvent at temperature T, and r_d is the radius of the diffusing molecule, which is calculated by the method of Edward[25a] and Bondi.[25b] Calculated r_d values are in good agreement with values obtained from ion mobility measurements.[26] The diffusion constant is proportional to temperature and inversely proportional to viscosity, whereas the viscosity also depends on temperature. On the basis of the temperature dependence of viscosities (Table 3), it can be estimated that the diffusion constant increases about 30% over the temperature range of our experiments, which means that the radical ions move 30% faster at 333 K than at 293 K. This increase in diffusion constant favors ion separation as the electron recombination through tunneling is unaffected by change in viscosity.

b. Dielectric Constants. The dependence of solvent dielectric constants on temperature follows a polynomial function. As the temperature increases from 293 to 333 K, the dielectric constant of DCE decreases from 10.37 to 8.45. The Onsager radius ($r_c = e^2/4\pi\epsilon_0\epsilon_S k_B T$), defined as the distance at which the Coulomb energy equals $k_B T$, increases from 55.6 Å at 293 K to 60.0 Å at 333 K. This makes it difficult for radical ion pairs to escape. Vauthey et al.[27] studied free ion formation at different temperatures by using time-resolved Raman spectra. The effect of temperature-induced change in viscosity of the solvent was analyzed. The fact that the polarity of a solvent at high temperatures is low was largely ignored. As far as the temperature-induced change in dielectric constant on free ion formation is concerned, it is important to mention that the impact is sensitive to the critical separation distance (r_m) at which decay and free ion formation happen. We intend to use values of free ion yields and their temperature dependence to probe the critical separation distances.

c. Influence of Temperature on Electron Recombination Rates. Electron recombination rate constants depend on temperature in a complicated manner. For radical ion pairs with a given separation distance, temperature-induced changes in static and optical dielectric constants cause a change in both driving force ($-\Delta G°$) and solvent reorganization energy (λ_s), which, in turn, affect the electron recombination rates. In principle, the effect of temperature on electron recombination rate can be understood from Marcus theory.[11] In the present work, recombination rates measured by transient photocurrent methods at each temperature will be used directly in the analysis.

For RIPs formed in a dielectric continuum, whose charge recombination occurs over a range of separation distances that can be predicted by the Marcus equation, a calculation method for escape probability has been developed.[28] The escape probability, Φ, defined as the total flux out of the sphere $4\pi r^2$ as $r \rightarrow \infty$ and $t \rightarrow \infty$, can be understood as the theoretical free ion yields. In these calculations, the fact that is usually ignored is that, for ion pairs formed after electron-transfer quenching, those that form free ions and those that are neutralized by electron recombination have different histories with different separation distributions. Equilibrium is not established during recombination or separation.[7] A Coulomb field in a structureless dielectric continuum is too simple to describe the interaction among the ion pairs, especially at short separation distances (from contact separation to a separation with one layer of solvent between donor and acceptor ions). Another disadvantage of using this kind of calculation in the analysis of the present results is that it is hard to establish a simple model for free ion formation based on the experimental data. The Onsager theory predicts the escape probabilities of geminate ion pairs of a given initial separation radius. It is widely used for the analysis of photo- and radiation-induced ionization in liquid solutions and solids. In the Onsager theory, the motion of the isolated ion pair is described by a Smoluchowski equation with a Coulomb term. The Onsager equation ($\Phi = e^{-r_c/r_0}$) thus obtained can be used to estimate the escape probability of ion pairs of initial radius r_0. The assumption of a continuum solvent model together with the boundary condition stating that there is a perfect sink at zero separation cannot fit the real situation. An extension to the Onsager treatment was developed by Hong and Noolandi (HN)[15] and Sano and Tachiya (ST).[16] In these treatments, they used a physical model similar to Onsager's except for a more realistic boundary condition assuming that the cation and the anion recombine with a finite rate at critical separation distance r_m. This boundary condition is normally called a partially reflective or Collins−Kimball boundary condition.[29] The escape probability, Φ, from this treatment is given by

$$\Phi = \frac{e^{-r_c/r_0} + (z-1)e^{-r_c/r_m}}{1 + (z-1)e^{-r_c/r_m}} \tag{2}$$

In eq 2, r_0 is the initial separation of the geminate ion pairs after electron-transfer quenching, r_c is the Onsager radius and $z = Dr_c/\kappa r_m^2$ where κ is the surface rate constant at critical separation r_m, with units of cm·s^{-1}. The surface rate constant κ is calculated by $\kappa = r_m/\tau$, where τ is the lifetime of the ion pairs concerned. When it is assumed that r_m is the separation at which recombination is in direct competition with free ion formation and that the potential energy beyond r_m is Coulombic, eq 2 offers a simple approach to understand the impact of separation distance on escape probability. The other great advantage of using eq 2 to estimate the escape probability is that it is related to a clear, simple physical picture and allows separate analysis of the effects of temperature-induced changes in solvent properties and rate constants of charge recombination. In real solutions, charge recombination occurs over a range of cation−anion distances rather than at some critical separation r_m. However, as the separation distance becomes larger, the recombination rates decay exponentially and make a smaller and smaller contribution to the overall recombination process. In this case, it is reasonable to consider r_m as the average separation distance at which recombination takes place.

Consider a typical system in our experiments: TIPB and DCA in the solvent DCE. The escape probabilities at different temperatures were calculated using eq 2 and then compared with the measured Y_{FRI}. Onsager radii of 55.6, 56.3, 57.3, 58.5, and and 60.0 Å are used in the calculation of escape probabilities

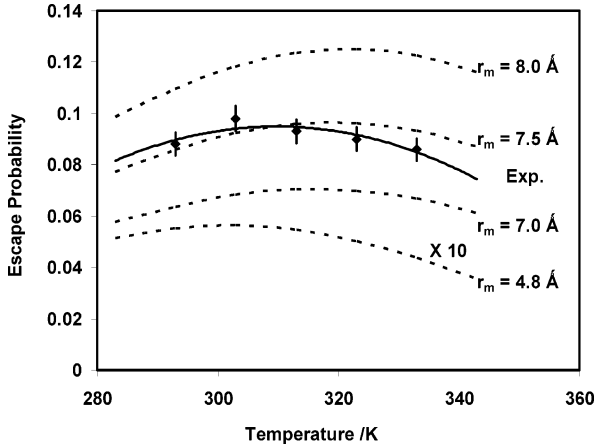

Figure 5. Comparison of calculated escape probability (Φ) of TIPB−DCA at different assumed r_m distances with the experimental Y_{FRI}. A r_m value of 7.5 Å gives escape probabilities that fit with experimental measurements with good agreement.

at 293, 303, 313, 323, and 333 K, respectively. Static dielectric constants (ϵ_s) are listed in Table 3. From 293 to 333 K, the viscosity of the solvent decreases from 0.83 to 0.52 mPa·s, which corresponds with a 40% increase in the diffusion constants of the radical ions. This makes a favorable contribution to the escape probability. On the other hand, the recombination rate obtained from the photocurrent rise time increases with temperature by about 10%, an unfavorable contribution to the escape probabilities of radical ion pairs. However, such a contribution is not large enough to account for the significant decrease in calculated escape probability at high temperatures. As temperature increases, the dielectric constant of the solvent decreases and makes ion pair separation more difficult than at low temperatures. The diffusion constant in eq 2 is the sum of those for the TIPB cation and DCA anion that are calculated from eq 1. Based on a spherical model, the molecular radii are 3.6 and 4.1 Å for DCA and TIPB, respectively. These calculations give overall diffusion constants of 1.36×10^{-9}, 1.61×10^{-9}, 1.88×10^{-9}, 2.17×10^{-9}, and 2.48×10^{-9} m^2 s^{-1} at 293, 303, 313, 323, and 333 K, respectively. The photocurrent rise time (τ) for TIPB−DCA can be determined to be 8.9 ns at 293 K and show very weak temperature dependence. These values are used in the calculation of surface rate constants ($\kappa = r_m/\tau$) and z values ($z = Dr_c/\kappa r_m^2$) at r_m in eq 2.

To calculate the escape probability by ST/HN equation, the only adjustable parameters are initial separation distance r_0 and the critical separation/recombination distance r_m. For a moderately polar solvent such as DCE, the effect of r_0 on the calculated escape probability is relatively small. We arbitrarily take r_0 to equal r_m in the calculation. The escape probability is sensitive to changes in r_m. Figure 5 shows the calculated escape probability of TIPB−DCA at different temperatures at preset r_m values of 4.8, 7.0, 7.5, and 8.0 Å. For comparison purposes, the experimental Y_{FRI} at different temperatures are also shown. It is clear that if r_m is set at 4.8 Å, which represents the separation distance of CRIPs for TIPB−DCA, the calculated escape probabilities are about 20 times less than experimentally determined Y_{FRI}. On the other hand, an r_m of 8.0 Å leads to escape probabilities that are much higher than that of experimental FRI yields.

The temperature dependence of the escape probability itself can also indicate the quality of choices of r_m. The Φ−T plot at r_m of 4.8 Å shows that Φ decreases significantly as temperature increases. This indicates that, at r_m of 4.8 Å, the separation of ion pairs is much less able to compete with recombination to give the measured Y_{FRI}. It also shows that, at a critical separation of 4.8 Å, escape probability is so sensitive to the temperature-induced decrease in dielectric constant that the calculated Φ does not fit the experimental results. Such results suggest that the critical separation must be larger than 4.8 Å. If r_m is increased to 7.0 Å, we find better agreement between the calculated escape probabilities and the experimental Y_{FRI} at all temperatures. But, the calculated escape probabilities are still less than those measured. Only when an r_m of 7.5 Å is used, which is near to the average face-to-face distance of SSRIPs of TIPB and DCA with a single layer of solvent molecules between them, can the calculated escape probabilities and the measured Y_{FRI} exhibit good agreement in both values and temperature dependence. For geminate ion pairs such as SSRIPs, it is reasonable to expect the Coulombic potential to give an accurate description of the interaction between cation and anion.[24] The above agreement suggests that the decay processes that are in direct competition with free ion formation are happening at single-layer solvent molecule separation distance. This also means that the potential barrier between CRIPs and SSRIPs is high enough to make them kinetically distinguishable species.

It is important to point out that the above analysis by itself does not provide further information on the mechanism of SSRIPs decay. Any process that prevents SSRIPs from forming free radical ions should be considered a decay channel. Such decay does not necessarily result in the direct formation of charge-neutralized donor and acceptor molecules. For example, the decay could proceed via back electron transfer through tunneling. It also could proceed via collapse to CRIPs by overcoming the barrier between SSRIPs and CRIPs. In other words, if CRIPs are unable to separate into SSRIPs because of their lower potential energy, as far as the decay of SSRIPs is concerned, collapse to CRIPs can be understood as the terminating step for SSRIPs, even if the CRIPs thus formed could live much longer than the SSRIPs.

The lifetimes (τ) of SSRIPs obtained from the photocurrent rise times are used to calculate surface rate constants (κ) and z parameters of eq 2. The lifetimes thus obtained reflect the total decay rate of SSRIPs. Theoretically, there are three components that may contribute to the decay processes of SSRIPs, i.e., collapse to CRIPs (k_{col}), recombination through tunneling (k_{-et}^{SSRIP}), and separation into free radical ions (k_{sep}) (Scheme 1). Assuming that collapse to CRIPs by overcoming the potential barrier between SSRIPs and CRIPs is the dominant pathway for the decay of SSRIPs, the virtual absence of any temperature dependence of free ion yields in the solvents used implies that the height of the potential barrier between SSRIPs and CRIPs is about the same as that between SSRIPs and free radical ions. Both the collapse of SSRIPs to CRIPs and the separation of SSRIPs into free radical ions are diffusive processes; apparent activation energies of both processes can be separated into an intrinsic term ($\Delta E^{\ddagger}$) and an additional term related to the temperature dependence of solvent viscosity (E_η).[27] Arrhenius expressions for the temperature dependence of the collapse (k_{col}) and the separation (k_{sep}) processes of SSRIPs can be written as[27]

$$k_{col} = AF(\eta)\exp\left(-\frac{\Delta E_{col}^{\ddagger}}{k_B T}\right) = A'\exp\left(-\frac{E_\eta + \Delta E_{col}^{\ddagger}}{k_B T}\right) \quad (3)$$

$$k_{sep} = BF(\eta)\exp\left(-\frac{\Delta E_{sep}^{\ddagger}}{k_B T}\right) = B'\exp\left(-\frac{E_\eta + \Delta E_{sep}^{\ddagger}}{k_B T}\right) \quad (4)$$

where $F(\eta) = \eta_0^{-1} \exp(-E_\eta/k_BT)$, A' (or B') $= A$ (or $B)\eta_0^{-1}$, and $\Delta E_{col}^{\ddagger}$ and $\Delta E_{sep}^{\ddagger}$ are the intrinsic activation energies for collapse and separation of SSRIPs, respectively. In DCE, E_η is estimated to be 0.25 eV by fitting the viscosities of DCE at different temperatures using $F(\eta) = \eta_0^{-1} \exp(-E_\eta/k_BT)$. The intrinsic activation barrier for the separation of SSRIPs into free radical ions is the electrostatic interaction within SSRIPs and can be estimated by

$$\Delta E_{sep}^{\ddagger} = \frac{e^2}{\epsilon_s r_{SSRIP}} \quad (5)$$

For DCE, the calculated potential barrier between SSRIPs and free radical ions is about 0.17 eV, assuming a charge separation distance of 7.5 Å for SSRIPs. The total apparent activation energy for both collapse ($E_\eta + \Delta E_{col}^{\ddagger}$) and separation ($E_\eta + \Delta E_{sep}^{\ddagger}$) processes would be about 0.42 eV. As temperature increases from 293 to 333 K, calculations based on eqs 3 and 4 give a more than 6-fold increase in the rate constants for collapse (k_{col}) and separation (k_{sep}). Our observation of no significant change in decay rate of SSRIPs as measured from the photocurrent rise time implies that neither of the approaches above is the dominant process for the decay of SSRIPs. As discussed in the previous section, another approach that might make a significant contribution to the decay of SSRIPs is a direct through-tunneling charge recombination without collapse to CRIPs. For decay of SSRIPs through tunneling, detailed analysis of the temperature dependence of rate constants can be conducted within the framework of Marcus theory. For each of the EDA systems studied in this work, there is an obvious difference between the decay rate of CRIPs as measured by single photon timing and that of SSRIPs as measured by transient photocurrent rise times. However, both decay rates exhibit similar weak temperature dependence. For CRIPs, a roughly 20% increase in decay rate is observed as the temperature increases from 293 to 333 K, whereas for SSRIPs, the increase is only about 10%. This is consistent with through-tunneling decay of SSRIPs. For the moderately polar solvents used in this work, the solvation energy gain is almost balanced by the electrostatic energy loss in going from SSRIPs to CRIPs. In this case, we cannot expect a significant impact of separation-distance-induced change in driving force on decay rate from CRIPs to SSRIPs. The solvent reorganization energy (λ_s) of SSRIPs is larger than that of CRIPs; this has an effect on the decay rates of the two species. However, it will do little to their temperature dependence. Actually, as we have seen experimentally, it will make the through-tunneling decay of SSRIPs exhibit even weaker temperature dependence compared to CRIPs.

When a flat donor such as DUR, which has approximately the same redox potential as TIPB, is used as the donor in DCE, the free ion yields are about 10-fold less than those with TIPB. However, as with TIPB, the free ion yield values exhibit very weak temperature dependence. This temperature dependence cannot be predicted from the escape probability calculation by simply using a small critical separation distance for DUR−DCA (Figure 5). Instead, the more than 10-fold decrease in measured free ion yield for DUR−DCA as compared with TIPB−DUR reflects the fact that approximately 90% of the quenching happens at a separation distance near contact and forms CRIPs, which make little or no contribution to free ion formation.

Conclusions

Free ion yields from geminate ion pairs formed after photoinduced electron transfer quenching are measured by transient photocurrent methods in three polar solvents. It was found that, generally, there is only a weak dependence of Y_{FRI} on temperature. An increase in temperature decreases the viscosity of the solvent and increases the mobility of cations and anions, making favorable contributions to the escape rates and Y_{FRI}. Quantitative analysis indicates that the observed weak dependence of free ion yields on temperature can be attributed to a decreased dielectric constant at higher temperature.

On the basis of the theoretical diffusion model developed by Hong and Noolandi and Sano and Tachiya under Collins-Kimball boundary conditions, parameters influencing free ion yields are analyzed, including dielectric constants, viscosities, initial separation distances of geminate ion pairs and changes in recombination rates. Escape probabilities of geminate ion pairs calculated at different initial formation and recombination separation distances are compared with experimental Y_{FRI}. This allows us to establish that free ions are mainly produced from SSRIPs that are initially formed after electron-transfer quenching. The calculation also implies that recombination through tunneling at separation distances of about 7.5 Å is the main decay process for SSRIPs. At that distance there is a direct competition between the tunneling recombination and separation processes of ion pairs.

Acknowledgment. We acknowledge support of this work from the Division of Chemical Science, Office of Basic Energy Sciences, U.S. Department of Energy, under grant DE-FG02-86ER13592.

References and Notes

(1) Eigen, M. *Nobel Lectures, Including Presentation Speeches and Laureates, Chemistry*; Elsevier: Amsterdam, 1972; pp 170.
(2) Winstein, S.; Robinson, G. C. *J. Am. Chem. Soc.* **1954**, *76*, 2597; **1956**, 78, 2767; **1956**, *78*, 2777; **1958**, *80*, 169.
(3) (a) Beens, H.; Weller, A. In *Organic Molecular Photophysics*; Birks, J. B. Ed.; Wiley: London, 1975; Vol. 2, Chapter 4. (b) Weller, A. *Z. Phys. Chem.* **1982**, *130*, 129.
(4) (a) *Photoinduced Electron Transfer*; Fox, M. A.; Chanon, M. Eds.; Elsevier: Amsterdam, 1988. (b) Gould, I. R.; Farid, S. *Acc. Chem. Res.* **1996**, *29*, 522. (c) Mataga, N.; Miyasaka, H. In *Electron Transfer − from Isolated Molecules to Biomolecules, Part 2*; Jortner, J., Bixon, M., Eds.; Advances in Chemical Physics; 1999; Vol. 107, p 431. (d) Barzykin, A. V.; Frantsuzov, P. A.; Seki, K.; Tachiya, M. In *Advances in Chemical Physics*; Prigogine, I., Rice, S. A., Eds.; Vol. 123; 2002; Vol. 123, p 511.
(5) (a) Gould, I. R.; Young, R. H.; Moody, R. E.; Farid, S. *J. Phys. Chem.* **1991**, *95*, 2068. (b) Gould, I. R.; Young, R. H.; Mueller, L. J.; Farid, S. *J. Am. Chem. Soc.* **1994**, *116*, 8176.
(6) Birks, J. B. *Photophysics of Aromatic Molecules*; Wiley: New York, 1970.
(7) Kavarnos, G. J.; Turro, N. J. *Chem. Rev.* **1986**, *86*, 401.
(8) Wiederrecht, G. P. In *Molecular and Supramolecular Photochemistry*; Ramamurthy, V., Schanze, K. S., Eds.; 2001; Vol. 7, p 319.
(9) Law, R.-Y. *Chem. Rev.* **1993**, *93*, 449.
(10) Mulliken, R. S.; Pearson, W. B. *Molecular Complexes: A Lecture and Leprint Volume*; Wiley: New York, 1969.
(11) Muller, P.-A.; Högemann, C.; Allonas, X.; Jacques, P.; Vauthey, E. *Chem. Phys. Lett.* **2000**, *326*, 321.
(12) (a) Mataga, N.; Okada, T.; Yamamoto, N. *Chem. Phys. Lett.* **1967**, *1*, 119. (b). Mataga, N.; Ezumi, K. *Bull. Chem. Soc. Jpn.* **1967**, *40*, 1355. (c) Mataga, N.; Murata, Y. *J. Am. Chem. Soc.* **1969**, *91*, 3144.
(13) Zhou, J.; Shah, R. P.; Findley, B. R.; Braun, C. L. *J. Phys. Chem.* **2002,** *106A*, 12.
(14) Zhou, J.; Findley, B. R.; Francis, T. M.; Nytko, E. A.; Braun, C. L. *Chem. Phys. Lett.* **2002**, *362*, 63.
(15) Hong, K. M.; Noolandi, J. *J. Chem. Phys.* **1978,** *68*, 5163.
(16) Sano, H.; Tachiya, M, *J. Chem. Phys.* **1979,** *71*, 1276.
(17) Zhou, J.; Findley, B. R.; Teslja, A.; Braun, C. L.; Sutin, N. *J. Phys. Chem.* **2000**, *104A*, 11512.
(18) Smirnov, S. N.; Braun, C. L. *Rev. Sci. Instrum.* **1998**, *69*, 2875.
(19) Hirata, Y.; Kanda, Y.; Mataga, N. *J. Phys. Chem.* **1983**, *87*, 1659.
(20) Marcus, R. A. *J. Chem. Phys.* **1956**, *24*, 966.
(21) Gould, I. R.; Farid, S. *J. Phys. Chem.* **1993**, *97*, 13067.
(22) Gould, I. R.; Ege, D.; Moser, J. E.; Farid, S. *J. Am. Chem. Soc.* **1990**, *112*, 4290.

(23) Zhou, J.; Findley, B. R.; Braun, C. L.; Sutin, N. *J. Chem. Phys.* **2001**, *114*, 10449.
(24) (a). Hilczer, M.; Tachiya, M. *Chem. Phys. Lett.*, **1998**, *295*, 337. (b). Kovalenko, A.; Hirata, F. *J. Phys. Chem*. **1999**, *103B*, 7942
(25) (a). Edward, J. T. *J. Chem. Educ*. **1970**, *47*, 262. (b). Bondi, A. *J. Phys. Chem*. **1964**, *64*, 441.
(26) Kim, S. K.; Burba, M. E.; Albrecht, A. C. *J. Phys. Chem*. **1994**, *98*, 9665.
(27) Vauthey, E.; Parker, A. W.; Nohova, B.; Phillips, D. *J. Am. Chem. Soc*. **1994**, *116*, 9182.
(28) Murata S.; Tachiya, M. *J. Chim. Phys.* **1996**, *93*, 1577.
(29) Collins, F. C.; Kimball, G. E. *J. Colloid Sci*. **1949**, *4*, 425.